

Polarons in cylindrical quantum wires

F. Buonocore

STMicroelectronics, Softcomputing/Nano-Organics/Si-Optics & Micromachining Operation, Stradale Primosole 50, I-95121 Catania, Italy

G. Iadonisi, D. Ninno, and F. Ventriglia

I.N.F.M. and Dipartimento di Scienze Fisiche, Università di Napoli Federico II, Complesso Universitario Monte S. Angelo, Via Cintia, I-80126 Napoli, Italy

(Received 16 October 2001; published 14 May 2002)

We present a study of polaron self-energies in a cylindrical quantum wire considering both volume and surface phonon modes in the dielectric continuum approximation. Full advantage is taken of the problem symmetries, and a generalization of the Lee-Low-Pines unitary transformation has been used. For the interaction with the volume phonon modes, we show that two opposite behaviors can be found for the self-energy as a function of the wire size, depending on whether or not the phonon modes are confined. These results are consistent with those concerning the mass renormalization and the first wire excited-state self-energy. Finally, we have also calculated the polaron self-energy for the electron–surface-phonon interaction showing that in this case the self-energy depends on the difference between the wire and embedding medium dielectric constants; it increases on reducing the wire size and can cross the volume confined polaron self-energy.

DOI: 10.1103/PhysRevB.65.205415

PACS number(s): 73.21.Hb, 71.38.–k, 63.22.+m

I. INTRODUCTION

An electron confined in a low-dimensional structure can interact with different species of phonons. When the confinement is structural as in deep-mesa-etched or grown structures, confined phonons and either surface or interface phonons should be considered when the confined structure is free standing or embedded in an other material, respectively.¹ Recent developments in epitaxial crystal growth techniques have made quantum wire (QW) nanostructures more and more important. A lot of attention has been paid to the electron-phonon interaction in these systems. The Hamiltonian for the electron-confined phonons interaction in rectangular QW's has been derived by Stroschio² following the calculation of confined modes in a dielectric slab discussed by Licari and Evrard,³ under the continuum dielectric (CD) approach. Polaron theory by using Stroschio's Hamiltonian has been developed.^{4,5} Confined phonons in cylindrical QW's in the CD approximation has been studied in Ref. 6. Confined and interface phonons interaction have been included by Li and Chen⁷ and by Xie *et al.*⁸ Enderlein⁹ employed the dispersive dielectric continuum model in order to study optical phonon modes in cylindrical QW's and calculated the Fröhlich interaction for confined and interface modes. The electron–surface-phonon interaction in cylindrical QW's has been studied by Sheng *et al.*¹⁰ Several authors have investigated the problem of an electron bound to an impurity and interacting with either bulk,^{11,12} using the so-called bulk-phonon approximation, or confined phonons.^{8,13,14} The effects of a magnetic field^{15–17} have also been considered. The problem of the screening due to an electron gas,^{18,19} and the band gap renormalization²⁰ have also been investigated.

In this paper we will focus our attention on the polaron renormalization effects due to the electron-phonon interaction in a cylindrical QW. We adopt a Lee-Low-Pines²¹ (LLP) approach modified in view of the cylindrical symmetry. In

fact, some translational symmetries are lost with respect to the infinite-medium case, and that will induce different Hamiltonian transformations in order to follow the idea of the LLP method. We shall choose a suitable form for the phonons distribution functions in order to calculate the polaron properties by means of a variational procedure. It is shown that the polaron ground-state self-energy as a function of the wire radius has two opposite behaviors according to whether phonons are confined or not. In particular, a confined electron interacting with unconfined phonons gives rise to a polaron self-energy which increases with decreasing the wire radius while the opposite occurs for a confined electron interacting with confined phonons. In the latter case, it is also shown that a crossing is possible between volume and surface polarons self-energies whose occurrence depends on the wire radius and the material dielectric constants.

II. MODEL AND THEORY

We consider the confined and interface electron-phonon interaction Hamiltonian calculated by Xie *et al.*⁸ in the CD approximation. This entails the following approximations: (1) the effective mass approximation for the electron, (2) the crystal is treated as continuous medium, (3) the dispersionless longitudinal confined phonon modes have vanishing electrostatic potential at the interfaces, (4) the interface phonon modes have the maximum electrostatic potential at the interfaces, and (5) the vibrations of the ions are harmonic. Choosing as z axis the wire longitudinal axis, the Fröhlich Hamiltonian is⁸

$$H = \frac{p^2}{2m^*} + \sum_{mlk_z} \hbar \omega_0 \left[a_{mlk_z}^\dagger a_{mlk_z} + \frac{1}{2} \right] - \sum_{mlk_z} \left[\Gamma_{LO}^{ml}(k_z) J_m \left(\frac{\chi_{ml} \rho}{R} \right) e^{im\varphi} e^{-ik_z z} a_{mlk_z}^\dagger + \text{H.c.} \right], \quad (1)$$

with

$$|\Gamma_{LO}^{ml}(k_z)|^2 = \frac{4e^2\hbar\omega_0}{LJ_{m+1}(\chi_{ml})^2(\chi_{ml}^2 + k_z^2 R^2)} \left(\frac{1}{\varepsilon_0} - \frac{1}{\varepsilon_\infty} \right), \quad (2)$$

where R is the wire radius, χ_{ml} is the l th zero of the Bessel function $J_m(x)$, ω_0 is the dispersionless frequency of the bulk longitudinal optical phonons, and finally ε_0 and ε_∞ are the static and high-frequency dielectric constants. An important dimensionless constant giving the interaction coupling strength is

$$\alpha = \frac{e^2}{2R_p} \left(\frac{1}{\varepsilon_0} - \frac{1}{\varepsilon_\infty} \right) / \hbar\omega_0,$$

where $R_p = \sqrt{\hbar/2m^*}\omega_0$ is the polaron radius. For instance, in gallium arsenide it is $\alpha = 0.07$ and $R_p = 4.0$ nm.

Because of the invariance for translations along the z axis and for rotations around the same axis, the total linear momentum

$$P_z = p_z + \sum_{mlk_z} \hbar k_z a_{mlk_z}^\dagger a_{mlk_z} \quad (3)$$

and the z component of the total angular momentum,

$$L_z = l_z + \sum_{mlk_z} m\hbar a_{mlk_z}^\dagger a_{mlk_z}, \quad (4)$$

commutes with the Hamiltonian (1). Here \vec{p} and \vec{l} are the electronic linear and angular momenta. These two commutation rules will give the opportunity of eliminating from the problem the electronic coordinates z and φ . We can achieve this with a sequence of unitary transformations. The first one is

$$H' = e^{-S_1} H e^{S_1}, \quad (5)$$

where the operator S_1 is defined as

$$S_1 = -i \sum_{mlk_z} k_z z a_{mlk_z}^\dagger a_{mlk_z}. \quad (6)$$

The second unitary transformation is

$$H_1 = e^{-S_2} H' e^{S_2}, \quad (7)$$

where

$$S_2 = -i \sum_{mlk_z} m\varphi a_{mlk_z}^\dagger a_{mlk_z}. \quad (8)$$

The last unitary transformation we use is that of Lee, Low, and Pines:²¹

$$H_2 = U^{-1} H_1 U, \quad (9)$$

with

$$U = \exp \left[\sum_{mlk_z} f_{ml}^*(k_z, \rho) a_{ml}(k_z) - f_{ml}(k_z, \rho) a_{ml}^\dagger(k_z) \right]. \quad (10)$$

Here $f_{ml}(k_z, \rho)$ are functions connected to the Fourier transform of the charge density and to the electron-phonon coupling. Since we are looking for the system ground state, H_2 can be averaged on the zero-phonon state $|0\rangle$ leading to

$$\langle 0 | H_2 | 0 \rangle = \frac{1}{2m^*} (p_\rho + J)^2 + G + \frac{1}{2m^*} [p_z^2 + p_\varphi^2 + K_z^2 + K_\varphi^2 - 2(K_z p_z + K_\varphi p_\varphi) + T + D], \quad (11)$$

where

$$K_z = \sum_{mlk_z} \hbar k_z |f_{ml}(k_z, \rho)|^2, \quad (12)$$

$$K_\varphi = \sum_{mlk_z} \frac{m\hbar}{\rho} |f_{ml}(k_z, \rho)|^2, \quad (13)$$

$$T = \sum_{mlk_z} \hbar^2 \left(k_z^2 + \frac{m^2}{\rho^2} \right) |f_{ml}(k_z, \rho)|^2, \quad (14)$$

$$D = \sum_{mlk_z} \hbar^2 \left| \frac{\partial f_{ml}(k_z, \rho)}{\partial \rho} \right|^2, \quad (15)$$

$$G = \sum_{mlk_z} \hbar\omega_0 |f_{ml}(k_z, \rho)|^2 - \sum_{mlk_z} \left[\Gamma_{LO}^{ml}(k_z) J_m \left(\frac{\chi_{ml}\rho}{R} \right) f_{ml}(k_z, \rho) + \text{c.c.} \right] \quad (16)$$

$$J = \frac{i\hbar}{2} \sum_{mlk_z} \left[f_{ml}(k_z, \rho) \frac{\partial f_{ml}^*(k_z, \rho)}{\partial \rho} - f_{ml}^*(k_z, \rho) \frac{\partial f_{ml}(k_z, \rho)}{\partial \rho} \right]. \quad (17)$$

Fortunately, Eq. (11) can be further simplified. Since $f_{mlk_z}(k_z, \rho)$ are either real or imaginary, it follows that $J = 0$. Moreover, $p_\varphi = l_z / \rho$ can be written as $M\hbar / \rho$ where $M\hbar$ is the angular momentum eigenvalue. Searching for electronic state with $M = 0$, we can set $p_\varphi = 0$. Finally, because of the wire symmetry, we have $f_{ml}(k_z, \rho) = f_{-ml}(k_z, \rho)$, and this implies that $K_\varphi = 0$. All that allows us to write Eq. (11) as

$$\langle 0 | H_2 | 0 \rangle = \frac{p_\rho^2 + p_z^2}{2m^*} + G + \frac{1}{2m^*} [K_z^2 - 2K_z p_z + T + D]. \quad (18)$$

At this point we can use as electron-phonon wave function

$$|\Psi\rangle = \Phi(\rho) \exp \left(\frac{i\varphi_z z}{\hbar} \right) |0\rangle, \quad (19)$$

where $\Phi(\rho)$ could be expressed as a linear combination of Bessel functions J_n . However, we are only interested in the ground and first excited electronic states: due to the large energy separation among the cylinder minibands, we neglect both the interactions between the ground and first electronic states and the interactions between these states and all higher

excited electronic states. For the ground state we have used a variational approach, with the following ansatz for the trial wave function: $\Phi(\rho)=0$ for $\rho \geq R$ and $\Phi(\rho) = N(1 - \rho^2/R^2)^\gamma$ for $\rho < R$ with γ the variational parameter. We note that for $\gamma=1.35$ the function $\Phi(\rho)$ fits $J_0(2.40482\rho/R)$ very well. On the contrary, for the first electronic excited state we have just used $J_1(3.8317\rho/R)$ without any variational parameter.

In order to determine $f_{ml}(k_z, \rho)$ we impose that the func-

tional variation of $E = \langle \Psi | H_2 | \Psi \rangle$ with respect to $f_{ml}^*(k_z, \rho)$ be zero—that is,

$$\frac{\delta \langle \Psi | H_2 | \Psi \rangle}{\delta f_{ml}^*} = 0. \quad (20)$$

A lengthy calculation leads to the following Eulerian equation:

$$-\frac{1}{|\Phi|^2} \frac{d|\Phi|^2}{d\rho} \frac{df_{ml}}{d\rho} - \frac{d^2 f_{ml}}{d\rho^2} + \left(\hbar^2 k_z^2 + \frac{\hbar^2 m^2}{\rho^2} + 2m^* \hbar \omega_0 \right) f_{ml} - [2\hbar k_z (\varphi_z - K_z)] f_{ml} = 2m^* \Gamma_{LO}^{ml}(k_z) J_m \left(\frac{\chi_{ml} \rho}{R} \right). \quad (21)$$

Unfortunately, contrary to other situations where we have been able to find an exact analytical solution of a differential equation of this type,^{22,23} to solve Eq. (21) is an hard task. We have therefore chosen a form for $f_{ml}(k_z, \rho)$ to be used within a variational calculation. An ansatz for $f_{ml}(k_z, \rho)$ can be constructed as following. First, one observes that neglecting the term D in Eq. (18), Eq. (20) leads to the following approximate expression for $f_{ml}(k_z, \rho)$:

$$\bar{f}_{ml}(k_z, \rho) = \frac{2m^* \Gamma_{LO}^{ml}(k_z) J_m \left(\frac{\chi_{ml} \rho}{R} \right)}{\left(\hbar^2 k_z^2 + \frac{\hbar^2 m^2}{\rho^2} + 2m^* \hbar \omega_0 \right) - 2\hbar k_z (\varphi_z - K_z)}. \quad (22)$$

This equation immediately suggests the ansatz

$$f_{ml}(k_z, \rho) = F_{ml}(k_z) \bar{f}_{ml}(k_z, \rho), \quad (23)$$

where $F_{ml}(k_z)$ are to be determined by the condition $\partial E / \partial F_{ml}^* = 0$. After some calculations we get

$$F_{ml}(k_z) = \frac{\left\langle \Gamma_{LO}^{ml}(k_z) J_m \left(\frac{\chi_{ml} \rho}{R} \right) \bar{f}_{ml}(k_z, \rho) \right\rangle}{\left\langle D_{ml}(k_z, \rho) |\bar{f}_{ml}(k_z, \rho)|^2 \right\rangle + \frac{\hbar^2}{2m^*} \left\langle \left| \frac{d\bar{f}_{ml}}{d\rho} \right|^2 \right\rangle + \frac{\hbar k_z}{m^*} \left\langle K_z |\bar{f}_{ml}(k_z, \rho)|^2 \right\rangle}, \quad (24)$$

with

$$D_{ml}(k_z, \rho) = \hbar \omega_0 + \frac{\hbar^2 k_z^2}{2m^*} + \frac{\hbar^2 m^2}{2m^* \rho^2} - 2\hbar \varphi_z k_z, \quad (25)$$

where we have used the abbreviation $\langle \dots \rangle = \langle \Phi | \dots | \Phi \rangle$. From Eq. (23) we obtain the expression of $f_{ml}(k_z, \rho)$, which characterizes the phonon distribution. In Eq. (23) we adopt a form for the phonon distribution functions $f_{ml}(k_z, \rho)$ which is somehow similar to the choice of Ref. 24 where excitons in polar semiconductors are studied. We are confident with the reliability of this variational approach because it led to results, for the case of excitons, in fair agreement with experimental data and with the results of more elaborate theories.²² The two systems—exciton in a bulk polar semiconductor and electron in a confined polar system—are investigatable with similar approaches because in both cases the phonons distribution functions have an explicit dependence on the spatial coordinates.

The total system energy is obtained by substituting again $f_{ml}(k_z, \rho)$ in E :

$$E = \frac{2(2\gamma+1)\gamma}{2\gamma-1} \left(\frac{R_p}{R} \right)^2 \hbar \omega_0 + \frac{\varphi_z^2}{2m^*} - \sum_{mlk_z} \frac{\left| \left\langle \Gamma_{LO}^{ml}(k_z) J_m \left(\frac{\chi_{ml} \rho}{R} \right) \bar{f}_{ml}(k_z, \rho) \right\rangle \right|^2}{\left\langle D_{ml}(k_z, \rho) |\bar{f}_{ml}(k_z, \rho)|^2 \right\rangle + \frac{\hbar^2}{2m^*} \left\langle \left| \frac{d\bar{f}_{ml}}{d\rho} \right|^2 \right\rangle + \frac{\hbar k_z}{m^*} \left\langle K_z |\bar{f}_{ml}(k_z, \rho)|^2 \right\rangle} - \sum_{mlk_z} \frac{\langle K_z^2 \rangle}{2m^*}. \quad (26)$$

The last two terms in Eq. (26) constitute the polaron self-energy ΔE .

The mass renormalization can be studied²² with the condition

$$\langle K_z \rangle = \eta \varphi_z, \quad (27)$$

from which we can obtain E with a variational calculation on the electronic state by minimizing E with respect to γ . Here η is a parameter that does not depend on φ_z and must be calculated self-consistently. Once this has been done, the polaron effective mass m_p can be obtained from the relation

$$\Delta E(\varphi_z) \equiv \Delta E(0) + \frac{\varphi_z^2}{2m^*} \left(1 - \frac{m^*}{m_p} \right).$$

The electron-surface phonon interaction can be studied with the Hamiltonian⁸

$$H = \frac{p^2}{2m^*} + \sum_{mk_z} \hbar \omega \left[b_{mk_z}^\dagger b_{mk_z} + \frac{1}{2} \right] - \sum_{mk_z} [\Gamma_{IO}^m(k_z) e^{im\varphi} e^{-ik_z z} b_{mk_z}^\dagger + \text{H.c.}] g_m(k_z \rho), \quad (28)$$

where

$$g_m(k_z \rho) = \begin{cases} K_m(k_z R) I_m(k_z \rho), & \rho \leq R, \\ I_m(k_z R) K_m(k_z \rho), & \rho > R, \end{cases} \quad (29)$$

$$|\Gamma_{IO}^m(k_z)|^2 = \frac{4e^2 \hbar \omega}{L K_m(k_z R)^2 I_m(k_z R) 2k_z R I_m'(k_z R)} \times \left(\frac{1}{\varepsilon - \varepsilon_0} - \frac{1}{\varepsilon - \varepsilon_\infty} \right), \quad (30)$$

$$\omega^2 = \left[1 + \frac{\varepsilon_0 - \varepsilon_\infty}{\varepsilon_\infty - \varepsilon} \right] \omega_{TO}^2, \quad (31)$$

$$\varepsilon = \frac{I_m(k_z R) K_m'(k_z R)}{I_m'(k_z R) K_m(k_z R)} \varepsilon_d, \quad (32)$$

and ε_d is the dielectric constant of the embedding medium. Following again the method of Ref. 21 and our variational procedure, we find that the polaron self-energy with $\varphi_z = 0$ is

$$\Delta E^{(S)} = - \sum_{mk_z} \frac{|\langle \Gamma_{IO}^m(k_z) g_m(k_z \rho) \bar{f}_m(k_z, \rho) \rangle|^2}{\langle d_m(k_z, \rho) | \bar{f}_m(k_z, \rho) \rangle^2 + \frac{\hbar^2}{2m^*} \left\langle \left| \frac{d\bar{f}_m}{d\rho} \right|^2 \right\rangle}, \quad (33)$$

where

$$\bar{f}_m = \frac{\Gamma_{IO}^m(k_z) g_m(k_z \rho)}{d_m(k_z, \rho)}, \quad (34)$$

$$d_m(k_z, \rho) = \hbar \omega + \frac{\hbar^2 k_z^2}{2m^*} + \frac{\hbar^2 m^2}{2m^* \rho^2}. \quad (35)$$

III. RESULTS AND DISCUSSION

Now we can discuss our numerical results. In panel (a) of Fig. 1 we plot the polaron ground-state self-energy with $\varphi_z = 0$. As can be seen, for $R > 4R_p$ the three-dimensional bulk limit $\Delta E = -\alpha \hbar \omega$ is recovered, while for $R \rightarrow 0$ the self-energy approaches zero. This result can easily be explained with the observation that by decreasing the radius, the volume of the effective material decreases until any medium to polarize is no longer available. However, in most polaron calculations the electron is considered as confined whereas the electron-phonon interaction is taken as that of an extended (bulk) system. This choice leads to the opposite behavior for the self-energy, as shown in panel (b) of Fig. 1. The Hamiltonian from which this result is derived is given in the Appendix. For instance, Erçelebi and Senger²⁵ and Pokalitev *et al.*²⁶ found indeed that approaching the one-dimensional limit the polaron self-energy increases, because the increase of the particle confinement implies an enhancement of the effective electron-phonon coupling. A similar effect can be found in the magnetopolaron theory.²³ The self-energy reduction with decreasing R shown in panel (a) of Fig. 1 highlights the peculiar behavior when the confined-electron–confined-phonon interaction is considered and should be the relevant effect in most either free-standing or embedded nanostructure.¹

In Fig. 2 we plot the polaron effective mass m_p with the coupling constant $\alpha = 0.1$ which is representative of an entire set of calculations. It can be seen from this figure that the polaron effective mass reduces, for a wire radius less than the polaron radius, to the electron effective mass m^* . Again

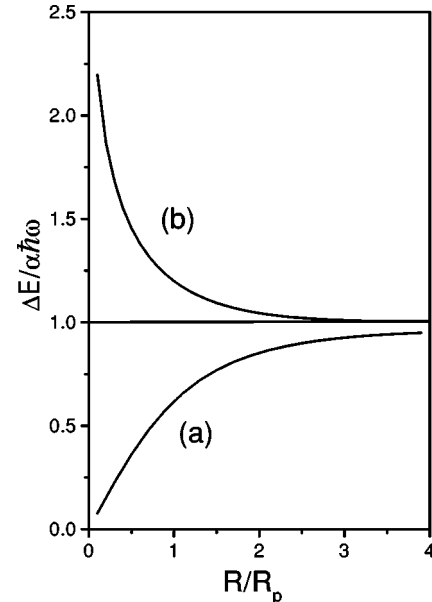


FIG. 1. The polaron ground-state self-energy as a function of the wire radius. In panel (a) the phonon modes are localized whereas in panel (b) they are delocalized.

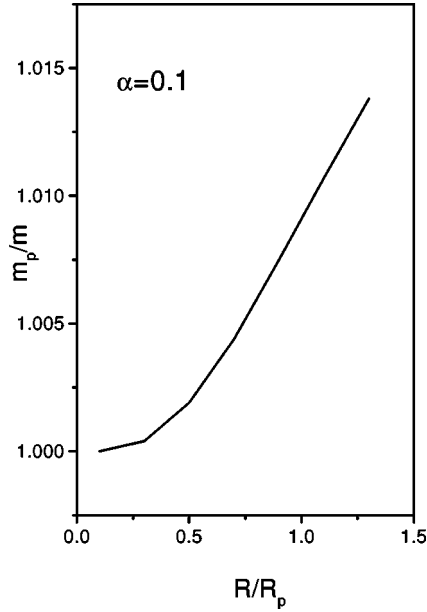


FIG. 2. The polaron effective mass as a function of the wire radius. The electron-phonon coupling constant is $\alpha=0.1$.

this finding, which is consistent with the polaron self-energy reduction, may have interesting consequences for free-standing nanostructures.

In Fig. 3 we present the results of a calculation in which we considered the first excited electronic state taking as $\Phi(\rho)$ in Eq. (19) the function $J_1(3.8317\rho/R)$ which is zero at the surface and it has a node on the wire center. The self-energy plotted is much smaller than that corresponding to the ground state [see panel (a) of Fig. 1]. This result reflects the nodal structure of the electronic wave function and indicates a polaron subband gap renormalization which tend to decrease with increasing energy.

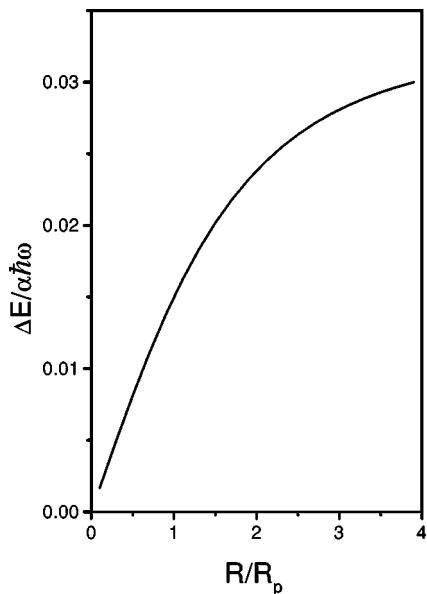


FIG. 3. The polaron self-energy for the first wire excited state as a function of the wire radius.

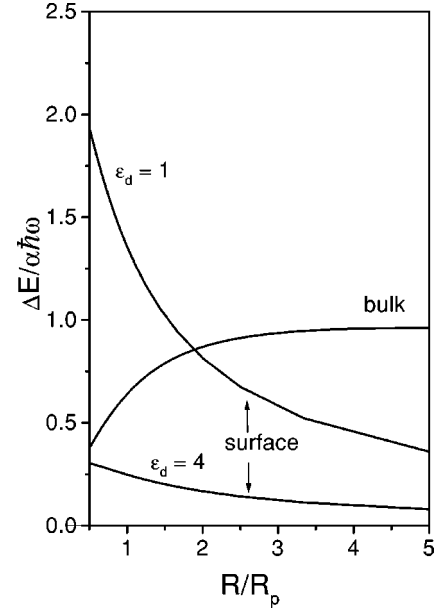


FIG. 4. Volume and surface polaron ground-state self-energy as a function of the wire radius. For surface phonons GaAs parameters have been used.

In Fig. 4 we present the last set of results in which we compare the self-energies due to both volume and surface polarons. As material parameters we have chosen those of GaAs considering two values of the embedding medium dielectric constant ($\epsilon_d=1$ and $\epsilon_d=4$). It is seen that the surface self-energy, contrary to the volume contribution, increases on reducing the wire radius. This effect, which is due to an increasing surface to volume ratio, implies a crossing between surface and volume self-energies at a value of R/R_p which depends on the value of the external dielectric constant ϵ_d . In any case, when strictly confined systems are considered, the surface renormalization effects can become dominants with a strength which depends on the external dielectric constant.

So far we have discussed our results within the framework of the standard CD model. A comparison with a modified CD model^{27,28} should not introduce, at first glance, changes in our conclusions. In fact, the interface phonon modes of the modified CD model agree with those of the standard model, in the zero-dispersion limit. Moreover, in our opinion, the corrections for the bulklike phonon modes introduced by the modified CD model could contribute to strengthen our results, due to the intermixing of the bulklike modes with the interface modes. However, the exact consequences of the modified CD model are beyond of the limits of the present paper and possibly they will be the subject of future work.

IV. SUMMARY

In this work we presented calculations on the polaron renormalization effects due to both the electron-surface and electron-volume phonon interactions in a cylindrical quantum wire with infinitely deep potential. A generalization of the Lee-Low-Pines method has been developed and a varia-

tional procedure has been followed. Universal curves have been calculated for the self-energies and for the mass renormalization. We have shown that two opposite behaviors for the polaron self-energy are obtained depending on whether or not the volume phonon modes are confined. For a free-standing nanostructure the self-energy significantly reduces for smaller sizes whereas just the opposite occurs when extended (bulk) phonon modes are considered.

The self-energy due to the interaction with surface phonons has been calculated showing that the self-energy strongly depends on both the difference between the wire and embedding medium dielectric constants and on the wire radius. Moreover, we have shown that there is the possibility, for certain values of dielectric constants and wire radius, of having a crossing between the volume and surface self-energies. Finally, decreasing the wire radius the renormalizations due to volume confined phonon may become less important of those due to surface phonons. The strength of this effect decreases when the dielectric constant of the embedding medium increases and approaches the value of the dielectric constant of the wire. We believe that these results may be relevant in the physics of colloiddally synthesized semiconductor nanocrystals¹ and in establishing their physical chemistry properties.²⁹

ACKNOWLEDGMENTS

Financial support from ENEA under Contract No. 2000/29324 is acknowledged.

APPENDIX

The Fröhlich Hamiltonian for a bulk polar material is

$$H = \frac{p^2}{2m^*} + \sum_{\vec{K}} \hbar \omega_0 a_{\vec{K}}^\dagger a_{\vec{K}} + \sum_{\vec{K}} (V_{\vec{K}} e^{i\vec{K} \cdot \vec{r}} a_{\vec{K}} + \text{H.c.}), \quad (\text{A1})$$

with

$$V_{\vec{K}} = \left[\frac{4\pi\alpha R_p}{SL} \frac{(\hbar\omega_0)^2}{k^2 + k_z^2} \right]^{1/2}, \quad (\text{A2})$$

where the phonon wave vector is $\vec{K} = (\vec{k}, k_z)$ and S is the normalization cross-sectional area and L its length. In order to rewrite Hamiltonian (A1) in cylindrical coordinates we transform canonically the boson operator $a_{\vec{K}}$ (which we write as $a_{\vec{k}, k_z}$) into the angular momentum representation

$$a_{k, k_z, m} = \sqrt{k} \left[\frac{S}{(2\pi)^2} \right]^{1/2} \int_0^{2\pi} \Theta_m^*(\varphi_{\vec{k}}) a_{\vec{k}, k_z} d\varphi_{\vec{k}}, \quad (\text{A3})$$

where

$$\Theta_m(\varphi) = \frac{1}{\sqrt{2\pi}} e^{im\varphi}. \quad (\text{A4})$$

Using Eq. (A3) and the expansion

$$e^{i\vec{k} \cdot \vec{\rho}} = 2\pi \sum_{m=-\infty}^{\infty} (i)^m J_m(k\rho) \Theta_m(\varphi) \Theta_m^*(\varphi_{\vec{k}}), \quad (\text{A5})$$

where $\varphi_{\vec{k}}$ is the \vec{k} polar angle, the Hamiltonian in Eq. (A1) becomes

$$H = \frac{p^2}{2m^*} + \sum_{mk_z} \int_0^\infty dk \hbar \omega_0 a_{k, k_z, m}^\dagger a_{k, k_z, m} + \sum_{mk_z} \int_0^\infty dk [V_{\vec{k}, k_z} T_{k, n}(\rho) \Theta_m(\varphi) \times e^{ik_z z} a_{k, k_z, m} + \text{H.c.}], \quad (\text{A6})$$

where

$$T_{k, m}(\rho) = \sqrt{kS} (i)^m J_m(k\rho).$$

The Hamiltonian of Eq. (A6) has been used with the confined ground electron state for the self-energy calculation whose results are shown in panel (b) of Fig. 1.

-
- ¹P. Moriarty, Rep. Prog. Phys. **64**, 297 (2001).
²M. A. Strosio, Phys. Rev. B **40**, 6428 (1989).
³J. J. Licari and R. Evrard, Phys. Rev. B **15**, 2254 (1977).
⁴W. S. Li, S. W. Gu, T. C. Au-Yeung, and Y. Y. Yeung, Phys. Rev. B **46**, 4630 (1992).
⁵K. D. Zhu and S. W. Gu, Solid State Commun. **80**, 307 (1991).
⁶N. C. Constantinou and B. K. Ridley, Phys. Rev. B **41**, 10 627 (1990).
⁷W. S. Li and C. Y. Chen, Physica B **229**, 375 (1997).
⁸H. J. Xie, C. Y. Chen, and B. K. Ma, Phys. Rev. B **61**, 4827 (2000).
⁹R. Enderlein, Phys. Rev. B **47**, 2162 (1993).
¹⁰W. D. Sheng, Y. Q. Xiao, and S. W. Gu, J. Phys.: Condens. Matter **5**, L129 (1993).
¹¹F. A. P. Osorio, M. H. Degani, and O. Hipolito, Phys. Rev. B **52**, 4662 (1995).
¹²I. Zorkani and L. Filali, Phys. Status Solidi B **215**, 999 (1999).
¹³E. P. Pokatilov, V. M. Fomin, S. N. Balaban, S. N. Klimin, and J. T. Devreese, Phys. Status Solidi B **210**, 879 (1998).
¹⁴D. S. Chuu, Y. N. Chen, and Y. K. Lin, Physica B **291**, 228 (2000).
¹⁵E. P. Pokatilov, S. N. Klimin, S. N. Balaban, and V. M. Fomin, Phys. Status Solidi B **189**, 433 (1995).
¹⁶T. Q. Lu, Y. S. Zheng, C. X. Zhang, and W. H. Wu, Phys. Status Solidi B **197**, 399 (1996).
¹⁷L. Wendler, Physica B **270**, 172 (1999).

- ¹⁸B. Tanatar, K. Güven, C. R. Bennett, and N. C. Constantinou, *Phys. Rev. B* **53**, 10 866 (1996).
- ¹⁹G. Q. Hai, F. M. Peeters, J. T. Devreese, and L. Wendler, *Phys. Rev. B* **48**, 12 016 (1993).
- ²⁰C. R. Bennett, K. Güven, and B. Tanatar, *Phys. Rev. B* **57**, 3994 (1998).
- ²¹T. D. Lee, F. Low, and D. Pines, *Phys. Rev.* **90**, 297 (1953).
- ²²G. Iadonisi, *Nuovo Cimento* **7**, 1 (1984).
- ²³D. Ninno and G. Iadonisi, *Phys. Rev. B* **39**, 10 963 (1989).
- ²⁴J. Pollmann and H. Büttner, *Phys. Rev. B* **16**, 4480 (1977).
- ²⁵A. Erçelebi and R. T. Senger, *Phys. Rev. B* **53**, 11 008 (1996).
- ²⁶E. P. Pokatilov, V. M. Fomin, J. T. Devreese, S. N. Balaban, and S. N. Klimin, *Physica E* **4**, 156 (1999).
- ²⁷K. Huang and B. Zhu, *Phys. Rev. B* **38**, 13 377 (1988).
- ²⁸R. Haupt and L. Wendler, *Phys. Rev. B* **44**, 1850 (1991).
- ²⁹L. E. Brus, *J. Chem. Phys.* **79**, 5566 (1983).